

# Intragenic Suppression of Trafficking-Defective KCNH2 Channels Associated with Long QT Syndrome<sup>S</sup>

Brian P. Delisle, Jessica K. Slind, Jennifer A. Kilby, Corey L. Anderson, Blake D. Anson, Ravi C. Balijepalli, David J. Tester, Michael J. Ackerman, Timothy J. Kamp, and Craig T. January

*Departments of Medicine and Physiology, University of Wisconsin, Madison, Wisconsin (B.P.D., J.K.S., J.A.K., C.L.A., B.D.A., R.C.B., T.J.K., C.T.J.); and Departments of Medicine, Pediatrics, and Molecular Pharmacology, Mayo Clinic College of Medicine, Rochester, Minnesota (D.J.T., M.J.A.)*

Received March 15, 2005; accepted April 25, 2005

## ABSTRACT

Mutations in the *KCNH2* or human *ether-a-go-go*-related gene-encoded K<sup>+</sup> channel reduce functional KCNH2 current (*I*<sub>KCNH2</sub>) to cause long QT syndrome (LQT2) by multiple mechanisms, including defects in intracellular transport (trafficking). Trafficking-deficient, or class 2, LQT2 mutations reduce the Golgi processing and surface membrane expression of KCNH2 channel proteins. Drugs that associate with pore-S6 intracellular drug binding domain of KCNH2 channel proteins to cause high-affinity block of *I*<sub>KCNH2</sub> also can increase the processing of class 2 LQT2 channel proteins through the secretory pathway. We used a strategy of intragenic suppression to test the hypothesis that amino acid substitutions in the putative drug

binding domain at residue Y652 could compensate for protein folding abnormalities caused by class 2 LQT2 mutations. We found that the Y652C substitution, and to lesser extent the Y652S substitution, resulted in intragenic suppression of the class 2 LQT2 G601S phenotype; these substitutions increased Golgi processing of G601S channel proteins. The Y652C substitution also caused intragenic suppression of the class 2 LQT2 V612L and F640V phenotypes but not the LQT2 N470D or F805C phenotypes. These are the first findings to demonstrate that a single amino acid substitution in the putative KCNH2 drug binding domain can cause intragenic suppression of several LQT2 mutations.

The *KCNH2* or the human *ether-a-go-go* related gene (*hERG*) encodes the  $\alpha$ -subunit channel proteins that oligomerize to form the pore of the cardiac rapidly activating delayed rectifier K<sup>+</sup> current, *I*<sub>Kr</sub> (Sanguinetti et al., 1995; Trudeau et al., 1995; Jones et al., 2004). More than 100 different KCNH2 mutations are associated with congenital long QT syndrome (LQT2; see <http://pc4.fsm.it:81/cardmoc/index.html>), and they are postulated to decrease *I*<sub>Kr</sub> by disrupting biophysical properties (gating/permeation), intracellular transport (trafficking) of KCNH2 channel proteins, or channel protein synthesis (Zhou et al., 1998; Delisle et al., 2004; Zhang et al., 2004).

WT KCNH2 channel proteins are synthesized and undergo core glycosylation in the endoplasmic reticulum, complex

glycosylation in the Golgi (Golgi processing), and then insert into the cell surface membrane to function. The “immature” core-glycosylated KCNH2 channel proteins have a molecular mass of ~135 kDa, and the “mature” complexly glycosylated KCNH2 channel proteins have a molecular mass of ~155 kDa (Zhou et al., 1998b; Petrecca et al., 1999; Gong et al., 2002). Several LQT2 mutations reduce the Golgi processing and insertion of KCNH2 channel proteins into the cell surface membrane, thereby decreasing KCNH2 current (*I*<sub>KCNH2</sub>) (Zhou et al., 1998a; Delisle et al., 2004). To date, 15 trafficking-deficient, or class 2 (Chugh et al., 2004; Delisle et al., 2004; Rossenbacker et al., 2005), LQT2 missense mutations (K28E, T65P, N470D, A561T, A561V, G601S, Y611H, V612L, T613M, L615V, R752W, F805C, V822M, R823W, and N861I) have been identified primarily by Western blot analysis, where the mature KCNH2 155-kDa protein band is absent or faint in appearance compared with the WT KCNH2 155-kDa protein band (Zhou et al., 1998, 1999; Furutani et al., 1999; Ficker et al., 2000a,b, 2002; Paulussen et al., 2002; Akhavan et al., 2003; Chugh et al., 2004). Cell culture conditions that “stabilize” protein conformation can increase Golgi processing and cell surface membrane expression for some class 2

This study was supported in part by Clinical Scientist Development Award from the Doris Duke Charitable Foundation (to M.J.A.) and National Heart, Lung, and Blood Institute grants F32-HL071476-01 (to B.P.D.), R01-HL6153 (to T.J.K.), and R01-HL60723 (to C.T.J.).

Article, publication date, and citation information can be found at <http://molpharm.aspetjournals.org>.  
doi:10.1124/mol.105.012914.

<sup>S</sup> The online version of this article (available at <http://molpharm.aspetjournals.org>) contains supplemental material.

**ABBREVIATIONS:** LQT2, long QT2; WT, wild-type; HEK, human embryonic kidney; I-V, current-voltage.

LQT2 channel proteins. For example, incubation in drugs that bind to intracellular pore-S6 residues, including Y652 and F656, to cause high-affinity block of  $I_{KCNH2}$  (Lees-Miller et al., 2000; Mitcheson et al., 2000; Fernandez et al., 2004) also increase the trafficking (pharmacological rescue) of the class 2 LQT2 K28E, T65P, N470D, and G601S channel proteins to the cell surface membrane (Zhou et al., 1999; January et al., 2000; Ficker et al., 2002; Paulussen et al., 2002; Gong et al., 2004; Rossenbacker et al., 2005). These data suggest that these drugs act as stabilizing ligands (Zhou et al., 1999; Deutsch C., 2003). They bind to the intracellular pore-S6 region of KCNH2 channel proteins to overcome abnormalities in protein folding and increase the processing of class 2 LQT2 channel proteins through the secretory pathway.

Intragenic suppression uses engineered secondary mutations (single amino acid substitutions) to identify regions that prevent protein dysfunction caused by a primary mutation (Papazian et al., 1995; Tiwari-Woodruff et al., 1997). There are two categories of intragenic suppression, those that nonselectively increase the overall stability of mutant proteins, and those that selectively compensate for structural interactions disrupted by the primary mutation. We used an intragenic suppression strategy to test the hypothesis that substitutions at Y652 could compensate for protein folding abnormalities that cause the class 2 LQT2 phenotype. Our data demonstrate that Y652C, and to a lesser extent Y652S, restores structural interactions that are important for KCNH2 channel protein processing in the secretory pathway.

## Materials and Methods

**WT KCNH2 and LQT2 Mutations.** WT KCNH2 and five different class 2 LQT2 channel mutations (N470D, G601S, V612L, F640V, or F805C) were studied. F640V is a novel KCNH2 mutation identified in a 49-year-old man with a prior history of syncope who collapsed with out-of-hospital cardiac arrest. Paramedics found the patient in ventricular fibrillation, and he was defibrillated 15 times to restore a normal heart rhythm. His electrocardiogram after recovery showed a markedly prolonged QT interval with a rate-corrected QT of 549 ms (normal <470 ms) and notched precordial T waves. The nucleotide change 1918T→G in the *KCNH2* gene, which causes the missense mutation F640V, was identified using polymerase chain reaction amplification, denaturing high-performance liquid chromatography, and DNA sequencing (Ackerman et al., 2003). The F640V mutation was identified in the patient's father and two of his siblings. One sibling is symptomatic for syncope, but the father and other sibling are asymptomatic. Two additional siblings collapsed suddenly and died before the age of 20 years and were never genotyped.

**KCNH2 Channel Protein Expression and Drug Exposure.** The appropriate nucleotide change 1918T→G was generated in WT KCNH2 cDNA in the pcDNA3 vector (Invitrogen, Carlsbad, CA) to generate the F640V construct. Similarly the appropriate nucleotide changes were made in WT KCNH2 cDNA to generate the Y652 substitutions Y652A, Y652H, Y652F, Y652S, or Y652C. For some experiments, the S620T engineered mutation (Ficker et al., 1998; Zhang et al., 1999) was incorporated into constructs that included the G601S mutation and/or the Y652C substitution. Constructs were stably or transiently expressed in human embryonic kidney (HEK) 293 cells as described previously (Zhou et al., 1998b, 1999). Western blot and electrophysiological analysis was done 48 h after transient expression. HEK293 cells were cultured in modified minimum Eagle's medium (Invitrogen) and kept at 37°C in 5% CO<sub>2</sub>. For experiments using pharmacological rescue, E4031 (10 μM; Alomone Labs,

Jerusalem, Israel), which causes high-affinity block of  $I_{KCNH2}$  (Zhou et al., 1998b), was added to the culture media for 24 h before Western blot analysis.

**Electrophysiology.**  $I_{KCNH2}$  was measured using the whole-cell patch-clamp technique as described previously (Delisle et al., 2003). The extracellular bath solution contained 137 mM NaCl, 4 mM KCl, 1.8 mM CaCl<sub>2</sub>, 1 mM MgCl<sub>2</sub>, 10 mM glucose, and 10 mM HEPES (pH 7.4 with NaOH), and the intracellular pipette solution contained 130 mM KCl, 1 mM MgCl<sub>2</sub>, 5 mM EGTA, 5 mM MgATP, and 10 mM HEPES (pH 7.2 with KOH). The Axopatch-200 patch clamp amplifier (Axon Instruments Inc., Union City, CA) was used to record  $I_{KCNH2}$  and to measure cellular capacitance. Pipettes had resistances between 1 and 2 MΩ, and the series resistance was compensated between 75 and 85%. Data were filtered at 10 kHz and were capacitance corrected. The pCLAMP 8.0 software (Axon Instruments Inc.) was used to generate voltage-clamp protocols, acquire  $I_{KCNH2}$  signals, and analyze data. Origin 6.0 (Origin-Lab Corp., Northampton, MA) was used for curve fitting and generating graphs. The holding potential in all experiments was −80 mV, and the baseline (zero current) is indicated as a dotted line in the figures. All voltage-clamp experiments were performed at 22–23°C within 1 to 2 h of removing the cells from their culture conditions.  $I_{KCNH2}$  was normalized to cell capacitance.

The following voltage protocols were used. 1) The peak tail  $I_{KCNH2}$  density was measured using a prepulse to a single voltage (50 mV to fully activated KCNH2 channel proteins) for 5 s followed by a test pulse to −120 mV for 3 s. 2) Voltage dependence of activation was measured as described previously (Anson et al., 2004). Cells were depolarized from −80 to 70 mV in 10-mV increments for 5 s, followed by a test pulse to −50 mV for 5 s. Current-voltage (I-V) relations were generated by plotting the peak outward tail  $I_{KCNH2}$  measured during the test pulse as a function of the prepulse voltage. The data were described using the Boltzmann equation to calculate the maximal current density ( $I_{\text{Density MAX}}$ ), the mid-point voltage of channel activation ( $V_{1/2}$ ), and the voltage range per *e*-fold change (*k*) in  $I_{KCNH2}$  (Delisle et al., 2003). The protocol was modified in cells expressing constructs that included the S620T mutation, where cells were only prepulsed from −80 to 10 mV. 3) The rate of  $I_{KCNH2}$  inactivation was measured using a three-pulse protocol as described previously (Anson et al., 2004). Cells were depolarized to 50 mV for 1.5 s, hyperpolarized to −100 mV for 2.5 ms, and then depolarized to test pulses between 0 and 90 mV in 10-mV increments for 1.5 s. The  $I_{KCNH2}$  decay generated during the test pulses was described as a single exponential process (correlation coefficient was typically >0.95) to calculate a time constant for channel inactivation ( $\tau_{\text{inact}}$ ). 4) The reversal potential ( $E_{\text{rev}}$ ) was calculated as described previously (Delisle and Satin, 2003). Cells were depolarized to 50 mV for 5 s to maximally activate KCNH2 channels, and then a test pulse to between −120 and −30 mV in 10-mV increments was applied. The peak tail  $I_{KCNH2}$  was plotted as a function of the test pulse voltage, and the  $E_{\text{rev}}$  was estimated by linearly extrapolating the zero current voltage.

**Western Blot.** HEK293 cells from similarly confluent cultures were used to isolate cell proteins. The Western blot procedure was similar, and the KCNH2 antibody was the same as to that described previously (Zhou et al., 1998b). Whole-cell lysates were generated by solubilizing cells in Nonidet P-40 buffer (Pierce Chemical, Rockford, IL). Equal amounts of protein were measured using Micro BCA protein assay reagent kit (Pierce Chemical) and subjected to either 7 or 7.5% SDS-polyacrylamide gel electrophoresis, and then the protein was electrophoretically transferred onto nitrocellulose membranes. The nitrocellulose membranes were incubated with a KCNH2 antibody directed against the C terminus. The antibody was then detected with the ECL detection kit (Amersham Biosciences Inc., Piscataway, NJ).

**Immunocytochemistry and Confocal Imaging.** Immunocytochemistry and confocal imaging were done as described previously (Delisle et al., 2003). HEK293 cells transiently expressing F640V or F640V/Y652C were plated in 35-mm Petri dishes containing collagen-coated coverslips. Cells were fixed with 4% buffered paraformaldehyde, permeabilized with 0.1% Triton X-100, and rinsed in 0.75%

glycine buffer to quench background fluorescence. The cells were then incubated at room temperature in blocking solution (10% goat serum, 0.05% NaN<sub>3</sub> in phosphate-buffered saline) for 1 h and subsequently supplemented with the KCNH2 antibody (1:3000). Excess antibody was washed off, and the cells were then incubated with highly cross-absorbed Alexa Fluor 568 goat anti-rabbit IgG (H+L) antibody (1:500; Molecular Probes, Eugene, OR). After washing with blocking solution, the coverslips were mounted on to a slide using 50% glycerol in phosphate-buffered saline. Imaging was performed with a Bio-Rad MRC 1024 laser scanning confocal microscope equipped with a mixed gas (Argon/Krypton) laser operated by 24-bit Lasersharpe software (Bio-Rad, Hercules, CA). Image acquisition used excitation at 568 nm with emission detected at  $605 \pm 16$  nm. Cells were randomly selected for imaging taken in 0.5- $\mu$ m sections. The number of Z-scan sections that were required to image a cell ranged between 15 and 25. Data are shown as single confocal images and as superimposed (stacked) Z-scan images.

**Statistics.** Data are presented as the mean  $\pm$  S.E. Student's *t* test is used for statistical analysis with *p* < 0.05 considered significant.

## Results

**Y652C and Y652S Substitutions Cause Intragenic Suppression of the Class 2 LQT2 G601S Phenotype.** Fig. 1 shows Western blot analysis of cells expressing WT KCNH2

channel proteins or the Y652 substitutions (–; left column), and cells expressing the LQT2 G601S mutation or the LQT2 G601S mutation with the Y652 substitutions (+; right column). Cells expressing WT KCNH2 channel proteins or the Y652 substitutions exhibited both the immature (135-kDa) and mature (155-kDa) protein bands. Cells expressing the G601S, G601S/Y652H, G601S/Y652F, or G601S/Y652A channel proteins exhibited only the immature (135-kDa) protein band typical of a class 2 LQT2 mutation. The important finding is that cells expressing the G601S/Y652C channel proteins, and to a lesser extent the G601S/Y652S channel proteins, exhibited both the immature (135-kDa) and mature (155-kDa) protein bands similar to WT KCNH2 channel proteins. These data demonstrate that the Y652C and Y652S substitutions caused intragenic suppression of the trafficking-deficient LQT2 G601S phenotype.

Figure 1B shows representative tail  $I_{KCNH2}$  traces recorded from cells expressing WT KCNH2, G601S, Y652C, or G601S/Y652C channel proteins, and it also shows mean peak tail  $I_{KCNH2}$  density measurements (Table 1). Compared with cells expressing WT KCNH2 channel proteins, peak mean tail  $I_{KCNH2}$  was reduced by 74% in cells expressing G601S channel proteins and by 77% in cells expressing the Y652C

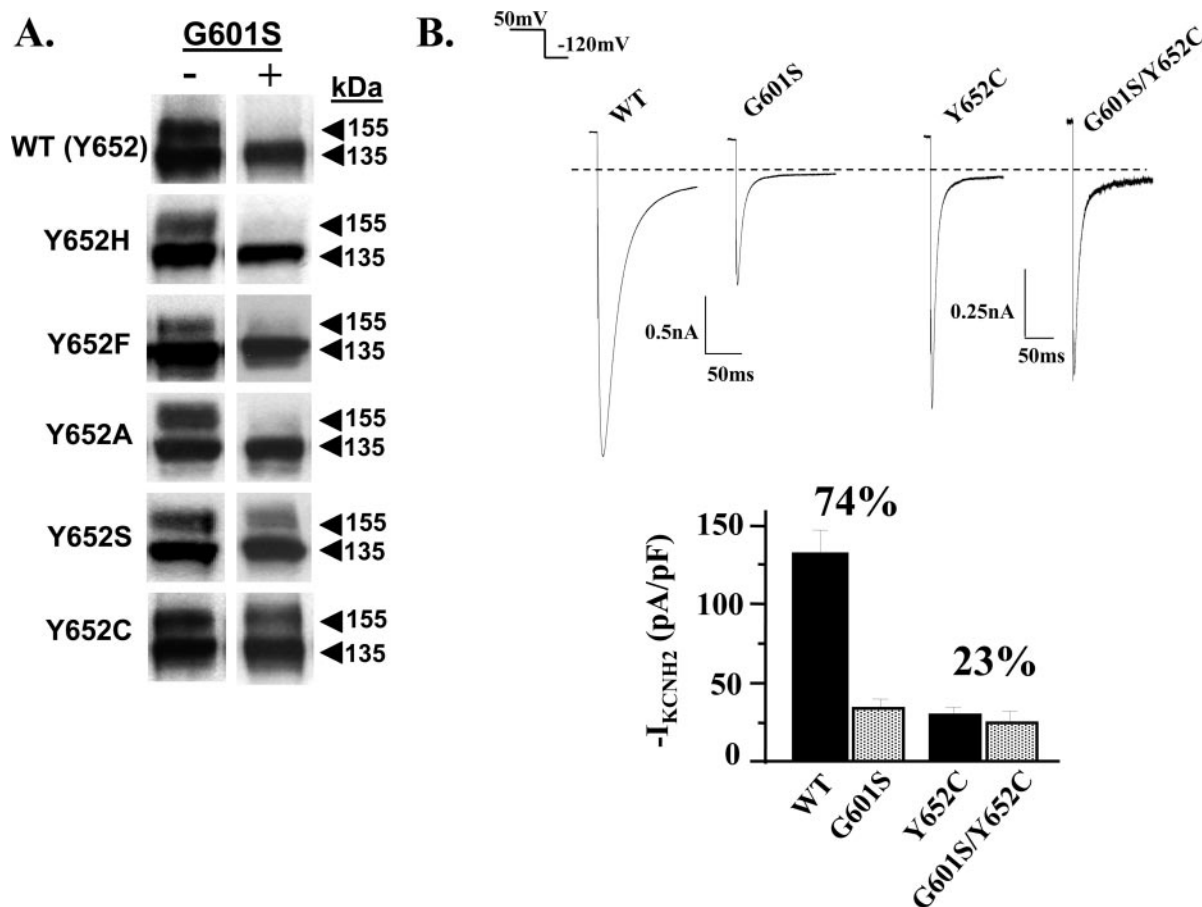


**Fig. 1.** Y652 substitutions differentially modify the class 2 LQT2 G601S phenotype. A, representative Western blot of cells expressing WT KCNH2 (Y652), Y652H, Y652F, Y652A, Y652S, or Y652C channel proteins without (–) or with (+) the G601S mutation. Cells expressing WT KCNH2, Y652H, Y652F, Y652A, Y652S, Y652C, G601S/Y652S, or G601S/Y652C channel proteins showed two KCNH2 protein bands at 135 and 155 kDa. Cells expressing G601S, G601S/Y652H, G601S/Y652F, or G601S/Y652A channel proteins have a single KCNH2 protein band at 135 kDa. B,  $I_{KCNH2}$  was measured in cells transiently expressing WT KCNH2, G601S, Y652C, or G601S/Y652C channel proteins. Representative tail  $I_{KCNH2}$  traces were recorded by applying a prepulse to 50 mV for 5 s and then a test pulse to –120 mV for 3 s. The graph shows the mean peak tail  $I_{KCNH2}$  recorded at –120 mV. Compared with cells expressing WT KCNH2 channel proteins, cells expressing G601S channel proteins caused a 74% reduction in  $I_{KCNH2}$ . Compared with cells expressing Y652C channel proteins, cells expressing G601S/Y652C channel proteins caused a 23% reduction in  $I_{KCNH2}$ .



substitution. Compared with cells expressing the Y652C substitution, the addition of the G601S mutation (G601S/Y652C) reduced peak mean tail  $I_{KCNH2}$  by only 23%. Because Y652C and G601S/Y652C channel proteins are processed similarly to WT KCNH2 channel proteins (Fig. 1A), we speculated that the Y652C substitution reduced  $I_{KCNH2}$  by altering biophysical properties of KCNH2 channels.

**The Y652C Substitution Reduced  $I_{KCNH2}$  and Altered KCNH2 Channel Gating.** Previous studies have shown that several different Y652 substitutions altered KCNH2 channel selectivity and/or gating (Mitcheson et al., 2000; Fernandez et al., 2004). To investigate the effects of the Y652C substitution on KCNH2 channel activation, the voltage dependence of activation was measured in cells expressing WT KCNH2 or Y652C channel proteins. Figure 2A shows representative families of  $I_{KCNH2}$  traces from cells expressing WT KCNH2 (left) or Y652C (right) channel proteins. Cells expressing WT KCNH2 channel proteins showed large-amplitude  $I_{KCNH2}$  that was minimally affected by the small-amplitude endogenous current present in our HEK293 cells (Zhou et al., 1998b). Cells expressing Y652C channel proteins showed smaller amplitude  $I_{KCNH2}$  that could not be isolated from the endogenous current in HEK293 cells, except during a test pulse to  $-50$  mV (inset). The peak mean endogenous HEK293 current measured in untransfected cells was  $29.5 \pm 4.7$  pA/pF during the prepulse to  $70$  mV and  $0.3 \pm 0.1$  pA/pF ( $n = 4$ ) during the corresponding test pulse to  $-50$  mV (Supplemental Fig. 1). Peak tail  $I_{KCNH2}$  recorded during the test pulse was plotted as a function of the prepulse voltage. Individual I-V relations were fit using a Boltzmann function to calculate  $I_{Density\ MAX}$ ,  $V_{1/2}$ , and  $k$ . The  $I_{Density\ MAX}$  was reduced in cells expressing Y652C channel proteins (WT,  $64.7 \pm 4.9$  pA/pF; Y652C,  $4.9 \pm 1.0$  pA/pF;  $n = 5-6$  cells;  $p < 0.05$ ), and there was a small difference in the  $k$  (WT,  $6.8 \pm 0.2$  mV/e-fold change; Y652C,  $6.0 \pm 0.5$  mV/e-fold change;  $p < 0.05$ ). There was no difference in the  $V_{1/2}$  (WT,  $-8.8 \pm 3.3$  mV; Y652C,  $-7.0 \pm 1.5$  mV). Figure 2A shows the mean peak tail  $I_{KCNH2}$  I-V relations with Boltzmann fits (solid line) measured from cells expressing WT KCNH2 (solid squares) or Y652C (open circles) channel proteins, which emphasizes the marked reduction in  $I_{KCNH2}$  by the Y652C substitution.

TABLE 1

Mean peak tail  $I_{KCNH2}$  values for cells expressing WT KCNH2 and Class 2 LQT2 channel proteins

Peak tail  $I_{KCNH2}$  measured in cells transiently expressing the WT KCNH2, G601S, F640V, or N470D channel proteins. The percentage reduction in the mean peak tail  $I_{KCNH2}$  for cells expressing the G601S, F640V, or N470D channel proteins compared with cells expressing WT KCNH2 channel proteins is given. Peak tail  $I_{KCNH2}$  was measured in cells transiently expressing the Y652C substitution, G601S/Y652C, F640V/Y652C, or N470D/Y652C channel proteins. The percentage reduction in the mean peak tail  $I_{KCNH2}$  for cells expressing the G601S/Y652C, F640V/Y652C, or N470D/Y652C channel proteins compared with cells expressing Y652C channel proteins is given.

	Peak Tail $I_{KCNH2}$	No. of Cells	$I_{KCNH2}$ Reduction
	pA/pF		%
WT	$-131.9 \pm 15.3$	22	
G601S	$-34.1 \pm 5.3$	15	74 <sup>a</sup>
F640V	$-8.4 \pm 1.3$	14	94 <sup>a</sup>
N470D	$-29.0 \pm 10.8$	9	78 <sup>a</sup>
Y652C	$-29.9 \pm 4.5$	14	
G601S/Y652C	$-25.0 \pm 7.3$	7	23 <sup>b</sup>
F640V/Y652C	$-22.0 \pm 1.6$	10	32 <sup>b</sup>
N470D/Y652C	$-8.8 \pm 1.8$	9	71 <sup>b</sup>

<sup>a</sup> Compared with WT.

<sup>b</sup> Compared with Y652C.

The kinetics of KCNH2 channel inactivation was measured using the three-pulse protocol. Figure 2B shows families of  $I_{KCNH2}$  traces recorded during test pulses in cells expressing WT (left) or Y652C (right) channel proteins, and it also shows the mean  $\tau_{inact}$  plotted as a function of the test pulse voltage for WT KCNH2 (■) or Y652C (○) channel proteins. At all voltages,  $\tau_{inact}$  calculated from cells expressing Y652C channels was faster than WT channel proteins (Fig. 2D;  $n = 5-6$  cells;  $p < 0.05$  at each voltage). These data demonstrate that the Y652C substitution enhanced the rate of inactivation of  $I_{KCNH2}$ . Because of the small  $I_{KCNH2}$  amplitude in cells expressing the Y652C substitution, a complete analysis of recovery from inactivation and deactivation kinetics, and single channel properties, were not determined.

To determine whether the Y652C substitution altered  $K^+$  selectivity, we calculated the  $E_{rev}$ . Figure 2C shows representative families of  $I_{KCNH2}$  traces recorded from cells expressing WT KCNH2 (left) or Y652C (right) channel proteins, and the mean peak tail  $I_{KCNH2}$  for cells expressing WT KCNH2 (■) or Y652C (○) channel proteins plotted as a function of the test pulse voltage. Cells expressing Y652C channel proteins did not show an altered  $E_{rev}$  when the data points were extrapolated to the zero current voltage (WT,  $-82 \pm 1$  mV; Y652C,  $-82 \pm 1$  mV;  $n = 6$  cells/group;  $p > 0.05$ ). These data suggest that the Y652C substitution does not alter KCNH2 channel selectivity.

Based on the Western blot (Fig. 1A) and biophysical (Fig. 2) analyses, our data suggest that Y652C and G601S/Y652C channel proteins traffic similar to WT KCNH2 channel proteins, but cells expressing KCNH2 channel proteins containing the Y652C substitution had small  $I_{KCNH2}$  levels because the Y652C substitution altered channel biophysical properties. Therefore, we studied intragenic suppression by Y652C in a model where inactivation gating was disrupted by the inclusion of the engineered mutation S620T.  $I_{KCNH2}$  recorded from cells expressing S620T channel proteins show minimal inactivation compared with cells expressing WT KCNH2 channel proteins (Ficker et al., 1998; Zhang et al., 1999). Figure 3A shows representative Western blot analysis ( $n = 3$ ) of cells transiently expressing S620T or S620T/Y652C channel proteins without (–; left column) or with (+; right column) the G601S mutation. Western blot analysis of cells expressing S620T, S620T/Y652C, or G601S/S620T/Y652C channel proteins showed that they were processed similar to WT KCNH2 channel proteins with both the immature (135-kDa) and mature (155-kDa) KCNH2 protein bands present. In contrast, Western blot analysis of cells expressing the G601S/S620T channel proteins showed a single protein band at 135 kDa, consistent with the class 2 LQT2 G601S phenotype. These data show that the addition of the Y652C substitution increased Golgi processing of the G601S/S620T channel protein, similar to that shown in Fig. 1A for G601S/Y652C. Figure 3B shows representative families of  $I_{KCNH2}$  traces recorded from cells expressing S620T, G601S/S620T, S620T/Y652C, or G601S/S620T/Y652C channel proteins using a 5-s prepulse from  $-80$  to  $10$  mV in  $10$ -mV increments, followed by a hyperpolarizing pulse to  $-50$  mV for  $5$  s. Because the S620T engineered mutation disrupted inactivation, cells expressing it had dramatically increased  $I_{KCNH2}$  amplitudes during depolarizing pulses (compare with WT in Fig. 2A). The addition of the G601S mutation (G601S/S620T) markedly reduced  $I_{KCNH2}$ . Cells expressing S620T/Y652C or

G601S/S620T/Y652C channel proteins also expressed large amplitude  $I_{KCNH2}$  during the depolarizing pulses. In addition, Fig. 3B shows the mean peak  $I_{KCNH2}$  amplitude measured at 10 mV from cells expressing S620T, G601S/S620T, S620T/Y652C, or G601S/S620T/Y652C channel proteins. The addition of the G601S mutation to S620T channel proteins reduced the  $I_{KCNH2}$  by 70%, whereas the addition of the G601S mutation to S620T/Y652C channel proteins reduced  $I_{KCNH2}$  by only 24%. By disrupting inactivation with the S620T engineered mutation, these results more clearly demonstrate that the Y652C substitution caused intragenic suppression of the class 2 LQT2 G601S phenotype.

**Y652C Caused Intragenic Suppression in Other Class 2 LQT2 Mutations.** Because G601S channel proteins exhibit pharmacological rescue, and the Y652 residue is important for high-affinity drug block of  $I_{KCNH2}$ , we determined whether there was a correlation between pharmacological rescue with E4031 and intragenic suppression by the Y652C substitution. Figure 4A shows Western blot analysis ( $n = 3-5$ ) of cells stably expressing the class 2 LQT2 mutations N470D, V612L, F640V, or F805C. The left column (–) shows the absence of the 155-kDa protein band typical of the class 2 LQT2 phenotype. The right column (+) shows that incubation of these cells in 10  $\mu$ M E4031 increased Golgi processing (155-kDa protein band) of N470D, V612L, and F640V, but not F805C channel proteins, and this is the first demonstration of pharmacological rescue of the V612L and F640V LQT2 channel proteins. Figure 4B shows Western blot analysis of

cells transiently expressing the N470D, V612L, F640V, or F805C without (–; left column) or with (+; right column) the Y652C substitution. The Y652C substitution increased the Golgi processing of the V612L and F640V channel proteins, but not the N470D or F805C channel proteins. Thus, although pharmacological rescue with E4031 and intragenic suppression with the Y652C substitution occurred jointly for some class 2 LQT2 mutations, as shown for the N470D mutation, there was not a one-to-one relationship. Mean peak tail  $I_{KCNH2}$  data for cells expressing WT  $KCNH2$ , G601S, F640V, and N470D channel proteins without or with the Y652C substitution are summarized in Table 1 (same protocol as in Fig. 1B). These electrophysiological data support the Western blot analysis shown in Fig. 4B. Compared with cells expressing WT  $KCNH2$  channel proteins, the mean peak tail  $I_{KCNH2}$  in cells expressing F640V channel proteins was reduced by 94%, consistent with its class 2 LQT2 phenotype. Compared with cells expressing Y652C channel proteins, cells expressing F640V/Y652C channel proteins reduced  $I_{KCNH2}$  by only 32%, consistent with intragenic suppression of its class 2 LQT2 phenotype. In contrast, for the N470D mutation, the Y652C substitution did not cause intragenic suppression, because cells expressing the N470D or N470D/Y652C channel proteins reduced mean peak tail  $I_{KCNH2}$  similarly (by 78 and 71% compared with their respective controls).

Class 2 LQT2 mutations result in the intracellular retention of channel protein in a perinuclear distribution (Zhou et

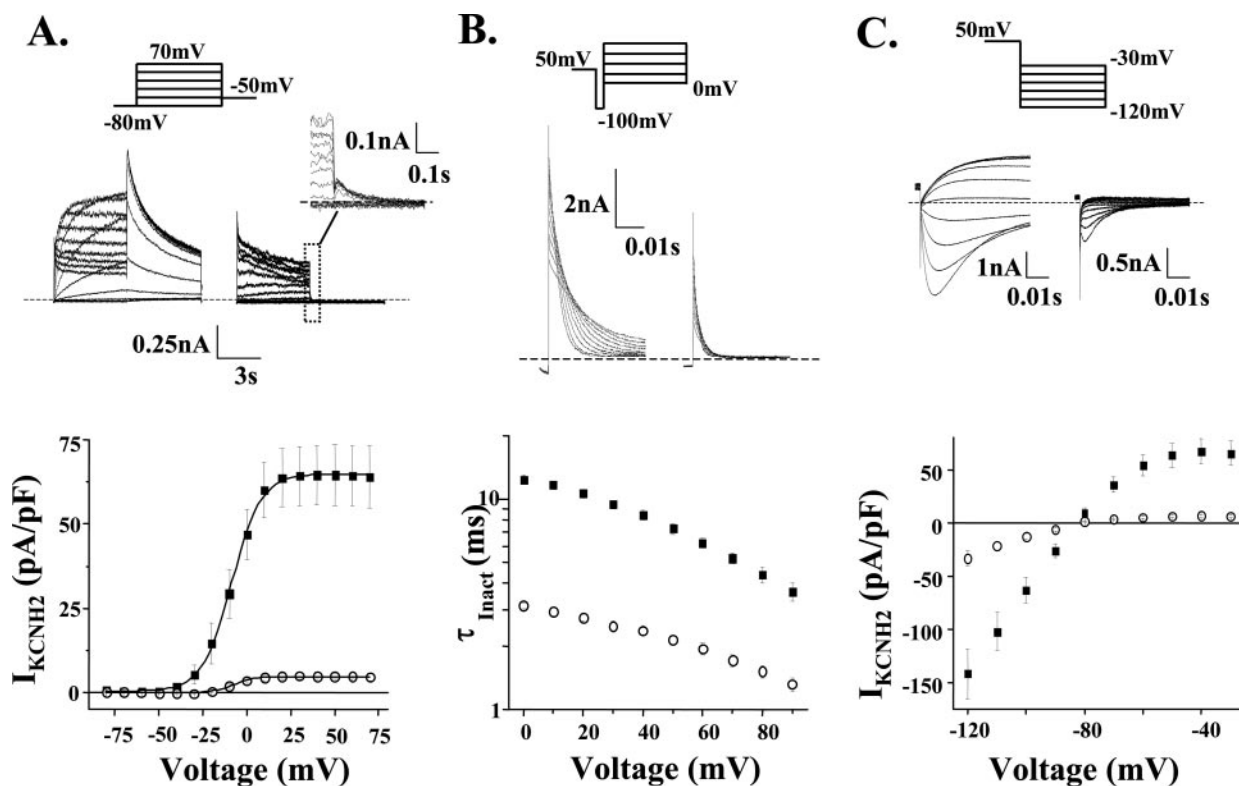


**Fig. 2.** Y652C substitution reduces  $I_{KCNH2}$  and accelerates inactivation kinetics. A, representative families of  $I_{KCNH2}$  recorded from cells expressing WT (left) or Y652C (right) channel proteins studied using voltage protocol shown (inset). The I-V relations showed the mean peak tail  $I_{KCNH2}$  for cells expressing WT (■) or Y652C (○) channel proteins plotted as a function of the prepulse voltage and described using a Boltzmann fit (solid lines). B, representative families of  $I_{KCNH2}$  recorded from cells expressing WT (left) or Y652C (right) channel proteins using the voltage protocol shown (inset). The mean  $\tau_{inact}$  was plotted as a function of the test pulse for cells expressing WT (■) or Y652C (○) channel proteins. C, representative families of tail  $I_{KCNH2}$  recorded from cells expressing WT (left) or Y652C (right) channel proteins were measured using the voltage protocol shown (inset). The mean peak tail  $I_{KCNH2}$  was plotted as a function of the test pulse voltage for cells expressing WT (■) or Y652C (○) channel proteins.

al., 1998a; Furutani et al., 1999; Ficker et al., 2000a,b; Paulussen et al., 2002; Akhavan et al., 2003; Delisle et al., 2003). We determined the subcellular localization of the F640V and F640V/Y652C protein using confocal microscopy. Figure 4C shows representative images of cells expressing F640V or F640V/Y652C channel proteins. The left column shows phase contrast images with the arrows, indicating cell surface membranes. The middle column shows the corresponding confocal image through the middle of the cells, and the right column shows a superimposed series of confocal Z-scan sections from the top to the bottom of the cells. These images show that F640V channel protein is found predominantly in a perinuclear pattern, whereas the F640V/Y652C protein distributes throughout the cell cytoplasm and the cell surface membrane ( $n = 7$  cells/group). These data provide additional support for the conclusion that the Y652C substitution causes intragenic suppression to improve channel protein processing through the secretory pathway.

**Y652C Reduces E4031 Sensitivity to  $I_{KCNH2}$  Block and Pharmacological Rescue.** Mutagenic modification of the Y652 residue has been previously shown to reduce the sensitivity of  $I_{KCNH2}$  to drug block. To confirm these findings in a mammalian expression system, we measured the E4031 sensitivity of  $I_{KCNH2}$  in cells expressing WT or Y652C channels using a protocol similar to that used in Fig. 1B. After obtaining control  $I_{KCNH2}$  data, 100 nM E4031 was added to the bath solution. In cells expressing WT channel proteins, E4031 decreased the peak tail  $I_{KCNH2}$  by  $83 \pm 1\%$  (Fig. 5A;  $n = 5$  cells). In contrast in cells expressing Y652C channel proteins, E4031 decreased  $I_{KCNH2}$  by  $22 \pm 3\%$  (Fig. 5A;  $n = 3$  cells). These findings are consistent with a decreased  $I_{KCNH2}$  sensitivity to block by E4031 for channel proteins with the Y652C substitution. Because the Y652C mutation

did not correct the processing of the N470D mutation (Fig. 4B), we determined whether the double mutation N470D/Y652C had altered sensitivity to pharmacological rescue by E4031. Western blot analysis demonstrated that incubation in E4031 (10  $\mu$ M for 24 h) increased KCNH2 channel protein processing in cells transiently expressing the N470D mutation but not in cells transiently expressing the N470D/Y652C double mutation (Fig. 5B;  $n = 3$ ). We also measured peak tail  $I_{KCNH2}$  similar to that done in Fig. 1B. E4031 incubation (10  $\mu$ M for 24 h) increased  $I_{KCNH2}$  in cells expressing N470D channel proteins by 179%, from  $-29.0 \pm 10.8$  (Table 1) to  $-80.8 \pm 25.8$  pA/pF ( $n = 7$ ). E4031 incubation of cells expressing N470D/Y652C channel protein resulted in a mean peak  $I_{KCNH2}$  of  $-12.0 \pm 2.7$  pA/pF ( $n = 5$ ), which was not statistically different ( $p > 0.05$ ) from the control value of  $-8.8 \pm 1.8$  pA/pF (Table 1). Likewise, in cells expressing G601S/Y652C or F640V/Y652C channel proteins, incubation in E4031 (10  $\mu$ M for 24 h) did not increase mean peak  $I_{KCNH2}$  [ $-26.4 \pm 3.5$  pA/pF ( $n = 6$ ) and  $-21.8 \pm 3.9$  pA/pF ( $n = 10$ ), respectively], compared with their control values (Table 1). We conclude that the Y652C mutation reduces the sensitivity of both drug block of WT  $I_{KCNH2}$  and pharmacological rescue.

## Discussion

Intragenic suppression has been used as an approach to identify domains that can compensate for structural perturbations caused by primary mutations (Papazian et al., 1995; Tiwari-Woodruff et al., 1997). High-affinity drug block of  $I_{KCNH2}$  depends on the association of the drugs with specific amino acids, including Y652. Because these drugs also can cause pharmacological rescue, we speculated that substitutions at Y652 could cause intragenic suppression of the class 2 LQT2 phenotype. We

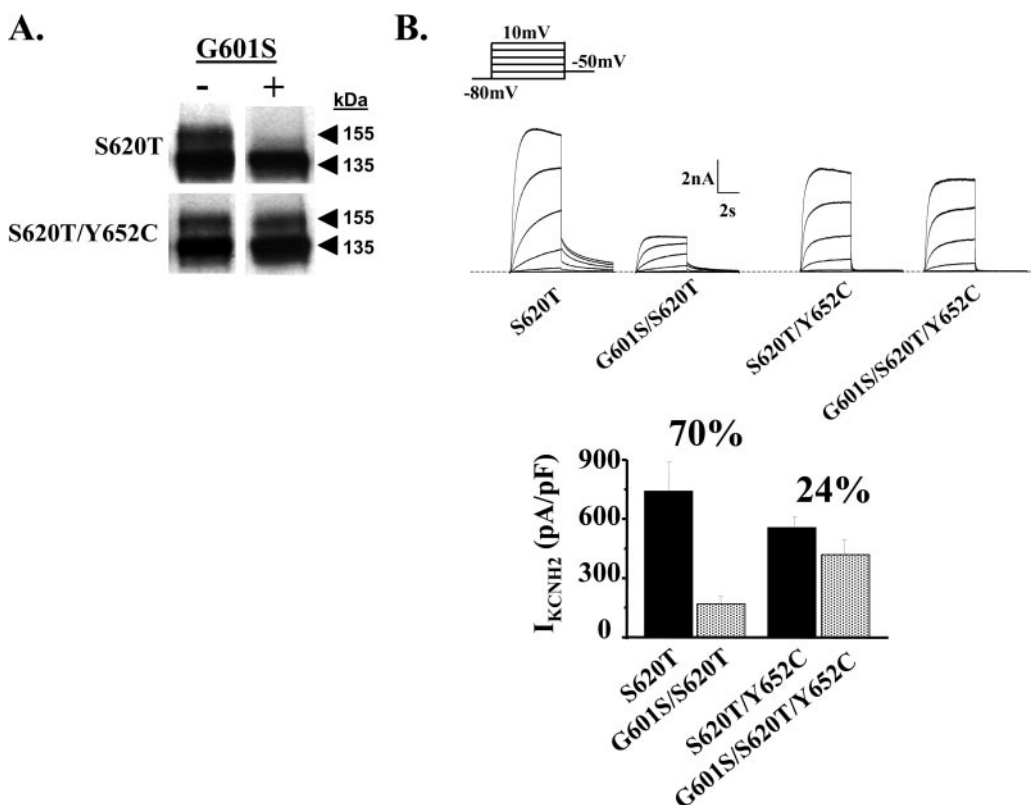


**Fig. 3.** Y652C caused intragenic suppression of G601S/S620T. A, top, Western blot analysis of cells expressing S620T or S620T/Y652C channel proteins without (-) or with (+) the G601S mutation. Cells expressing S620T, S620T/Y652C, or G601S/S620T/Y652C channel proteins showed two KCNH2 protein bands at 135 and 155 kDa. Cells expressing G601S/S620T channel proteins have a single KCNH2 protein band at 135 kDa. B, representative families of  $I_{KCNH2}$  recorded from cells expressing S620T, S620T/Y652C, G601S/S620T, or G601S/S620T/Y652C channels studied using the voltage protocol shown (inset). The graph shows the mean peak  $I_{KCNH2}$  measured at 10 mV for cells expressing S620T, G601S/S620T, S620T/Y652C, or G601S/S620T/Y652C channel proteins. Compared with cells expressing S620T channel proteins, cells expressing G601S/S620T channel proteins caused a 70% reduction in  $I_{KCNH2}$ . Compared with cells expressing S620T/Y652C channel proteins, cells expressing G601S/S620T/Y652C channel proteins caused only a 24% reduction in  $I_{KCNH2}$ .



found that the Y652C substitution caused intragenic suppression of the class 2 LQT2 G601S, V612L, and F640V phenotypes and that the Y652S substitution also caused intragenic suppression of the class 2 LQT2 G601S phenotype. For the N470D LQT2 mutation, we were able to dissociate intragenic suppression and pharmacological rescue. This demonstrates that intragenic suppression by amino acid substitutions at Y652 and pharmacological rescue do not act identically and raises the

possibility that pharmacological rescue may correct the class 2 LQT2 phenotype by more than one mechanism. Further experiments using substitutions at different residues important for high-affinity drug block of  $I_{KCNH2}$ , such as F656, are currently being investigated.

Distinct steps in the assembly and folding of Shaker  $K^+$  channel proteins during biogenesis have been identified using engineered missense mutations and deletions (Schulze et al.,

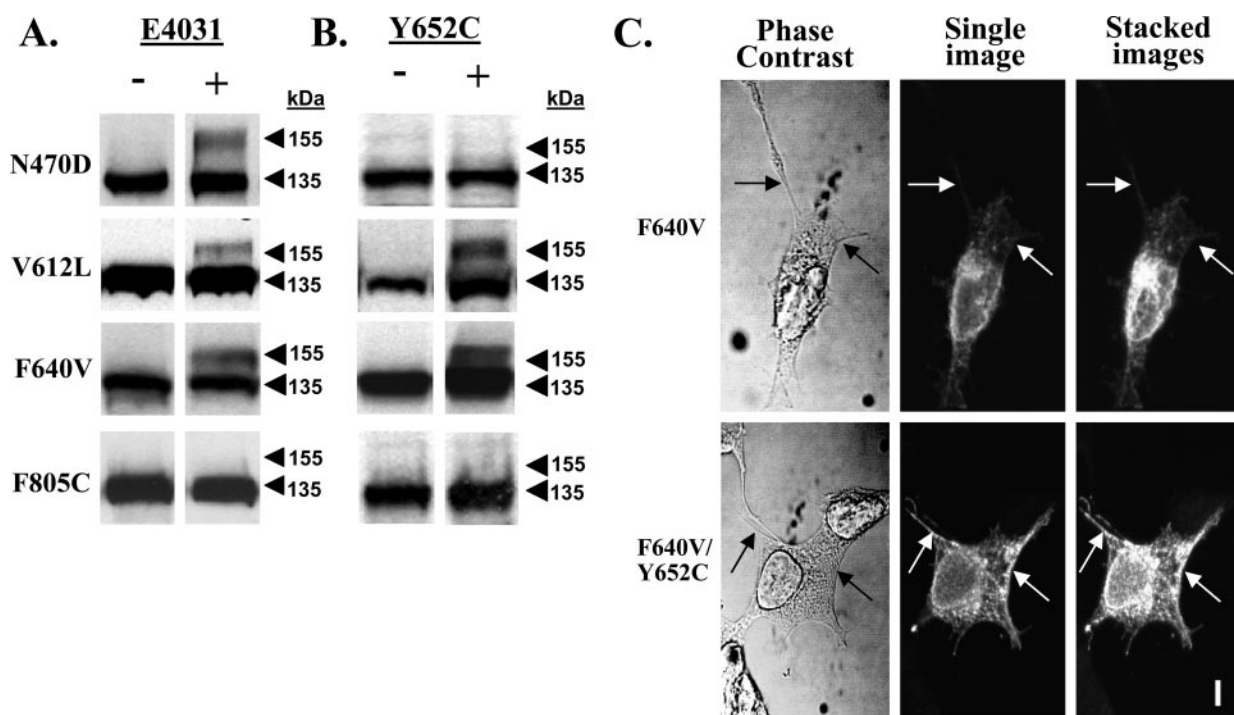


**Fig. 4.** Y652C substitution caused intragenic suppression of the class 2 LQT2 V612L and F640V phenotype. A, Western blot analysis of cells stably expressing the N470D, V612L, F640V, or F805C channel proteins cultured incubated without (-) or with E4031 (24 h; +). In the absence of E4031, a single protein band was present at 135 kDa. In cells expressing the N470D, V612L, or F640V channel proteins, incubation in E4031 caused the appearance of a second protein band at 155 kDa. B, representative Western blots analysis of cells transiently expressing the N470D, G601S, V612L, or F805C channel proteins without (-) or with (+) the Y652C substitution. Cells expressing N470D, G601S, V612L, F805C, N470D/Y652C, or Y652C/F805C channel proteins showed a single protein band at 135 kDa. Cells expressing V612L/Y652C or F640V/Y652C had two protein bands at 135 and 155 kDa. C, left column shows phase contrast images of the cells expressing F640V or F640V/Y652C channel proteins to visualize the cell surface membrane (arrows). The middle column shows a single confocal section through the middle of each cell. The right column shows a superimposed stacked series of Z-scan confocal images from the top to the bottom of the each cell. Scale bar (bottom right image), 1  $\mu$ m.

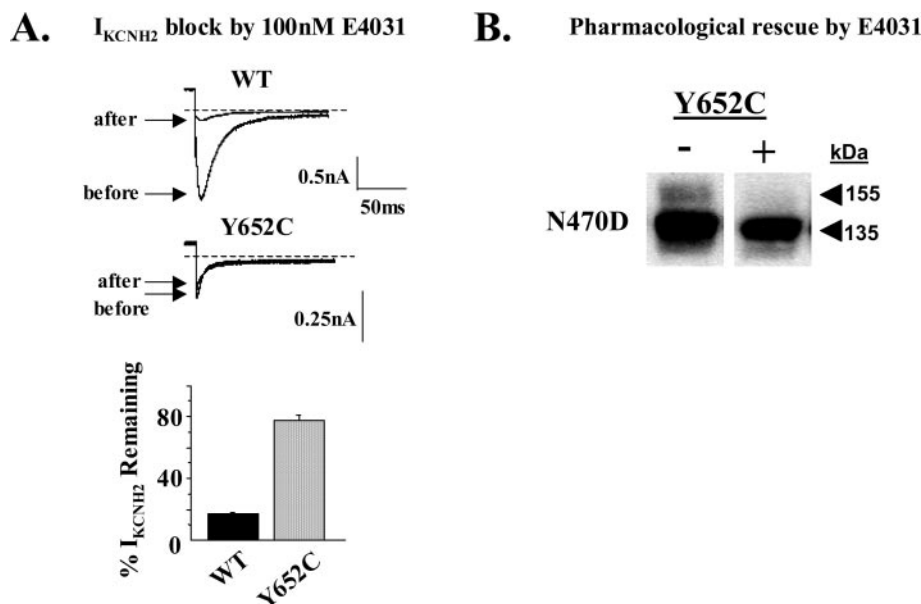


**Fig. 5.** Y652C mutation reduces the sensitivity of both drug block of WT  $I_{KCNH2}$  and pharmacological rescue of the N470D mutation. A, E4031 sensitivity of  $I_{KCNH2}$  in WT or Y652C expressing cells was determined using a protocol similar to Fig. 2B. After obtaining initial  $I_{KCNH2}$  amplitudes (before), 100 nM E4031 was added to the bath solution (after). In WT cells, E4031 decreased the peak tail  $I_{KCNH2}$  by  $83 \pm 1\%$ , whereas in Y652C cells E4031 decreased  $I_{KCNH2}$  by  $22 \pm 3\%$ . B, Western blot analysis of cells transiently expressing the N470D (-) or N470D/Y652C channel proteins (+) incubated in 10  $\mu$ M E4031 for 24 h. Cells expressing the N470D channel proteins had two protein bands at 135 and 155 kDa, whereas cells expressing the N470D/Y652C channel proteins showed a single protein band at 135 kDa.

1998). The proposed sequence of events during Shaker K<sup>+</sup> channel biogenesis in the endoplasmic reticulum are as follows: 1) membrane insertion and core glycosylation, 2) assembly of Shaker  $\alpha$ - and  $\beta$ -subunit channel proteins, 3) formation of the pore and voltage sensor, and 4) formation of proximity between adjacent amino and carboxyl termini. Assuming a similar sequence of events for KCNH2 channel proteins, we suggest that class 2 LQT2 mutations are capable of disrupting different steps in KCNH2 channel biogenesis to cause the class 2 or trafficking deficient LQT2 phenotype. Using this scheme, we propose that intragenic suppression and pharmacological rescue are able to compensate for disrupted structural interactions of some LQT2 mutations that occur during later steps in KCNH2 biogenesis. This is supported by the observations that 1) LQT2 mutations that do not undergo intragenic suppression or pharmacological rescue (i.e., F805C) do not cause dominant negative suppression of WT KCNH2 channel proteins (Ficker et al., 2002), suggesting that these class 2 LQT2 mutations disrupt biogenesis before the oligomerization step(s); 2) class 2 LQT2 mutations that do undergo pharmacological rescue show dominant negative suppression of WT KCNH2 channel proteins (Gong et al., 2004), suggesting that these class 2 LQT2 mutations disrupt biogenesis steps after oligomerization; and 3) the pore 5 residue Y652C selectively caused intragenic suppression of the class 2 LQT2 phenotype for mutations in the extracellular region of the pore, suggesting that G601S, V612L, and F640V prevent the proper formation of the KCNH2 channel pore to cause the class 2 LQT phenotype. The N470D mutation did not show intragenic suppression with the Y652C substitution but showed pharmacological rescue, potentially because this mutation disrupts other steps late in KCNH2 biogenesis, such as the folding of the voltage sensor or the formation of proximity between adjacent amino and carboxyl termini.

These are the first data to show intragenic suppression of the class 2 LQT2 phenotype. Our data were obtained in a human K<sup>+</sup> channel disease model, and resemble previous findings in Shaker K<sup>+</sup> channels obtained using engineered mutations (Papazian et al., 1995; Tiwari-Woodruff et al., 1997). These data demonstrate that residue substitution in the putative drug binding domain of the KCNH2 channel pore can compensate for structural interactions disrupted by multiple class 2 LQT2 mutations located in the extracellular region of the pore. These mutations (G601S, V612L, and F640V) also undergo pharmacological rescue, thus drug binding to Y652 may also facilitate proper pore formation, thereby explaining one potential mechanism by which pharmacological rescue occurs. Because the N470D mutation does not undergo intragenic suppression but does undergo pharmacological rescue, we suggest that different mechanisms may underlie the pharmacological rescue of class 2 LQT2 mutations located in different regions of the KCNH2 channel protein.

## References

- Ackerman MJ, Tester DJ, Jones G, Will ML, Burrow CR, and Curran ME (2003) Ethnic differences in cardiac potassium channel variants: implications for genetic susceptibility to sudden cardiac death and genetic testing for congenital long QT syndrome. *Mayo Clin Proc* **78**:1479–1487.
- Akhavan A, Atanasiu R, and Shrier A (2003) Identification of a COOH-terminal segment involved in maturation and stability of human ether-a-go-go-related gene potassium channels. *J Biol Chem* **278**:40105–40112.
- Anson BD, Ackerman MJ, Tester DJ, Will ML, Delisle BP, Anderson CL, and January CT (2004) Molecular and functional characterization of common polymorphisms in HERG (KCNH2) potassium channels. *Am J Physiol* **286**:H2434–H2441.
- Chugh SS, Senashova O, Watts A, Tran PT, Zhou Z, Gong Q, Titus JL, and Hayflick SJ (2004) Postmortem molecular screening in unexplained sudden death. *J Am Coll Cardiol* **43**:1625–1629.
- Delisle BP, Anderson CL, Balijepalli RC, Anson BD, Kamp TJ, and January CT (2003) Thapsigargin selectively rescues the trafficking-defective LQT2 channels G601S and F805C. *J Biol Chem* **278**:35749–35754.
- Delisle BP, Anson BD, Rajamani S, and January CT (2004) Biology of cardiac arrhythmias: ion channel protein trafficking. *Circ Res* **94**:1418–1428.
- Delisle BP and Satin J (2003) Monovalent cations contribute to T-type calcium channel (Cav3.1 and Cav3.2) selectivity. *J Membr Biol* **193**:185–194.
- Deutsch C (2003) The birth of a channel. *Neuron* **40**:265–276.
- Fernandez D, Ghanta A, Kauffman GW, and Sanguinetti MC (2004) Physicochemical features of the hERG channel drug binding site. *J Biol Chem* **279**:10120–10127.
- Ficker E, Dennis AT, Obejero-Paz CA, Castaldo P, Taglialatela M, and Brown AM (2000a) Retention in the endoplasmic reticulum as a mechanism of dominant-negative current suppression in human long QT syndrome. *J Mol Cell Cardiol* **32**:2327–2337.
- Ficker E, Jarolimek W, Kiehn J, Baumann A, and Brown AM (1998) Molecular determinants of dofetilide block of HERG K<sup>+</sup> channels. *Circ Res* **82**:386–395.
- Ficker E, Obejero-Paz CA, Zhao S, and Brown AM (2002) The binding site for channel blockers that rescue misprocessed human long QT syndrome type 2 ether-a-go-go-related gene (HERG) mutations. *J Biol Chem* **277**:4989–4998.
- Ficker E, Thomas D, Viswanathan PC, Dennis AT, Priori SG, Napolitano C, Memmi M, Wible BA, Kaufman ES, Iyengar S, et al. (2000b) Novel characteristics of a misprocessed mutant HERG channel linked to hereditary long QT syndrome. *Am J Physiol* **279**:H1748–H1756.
- Furutani M, Trudeau MC, Hagiwara N, Seki A, Gong Q, Zhou Z, Imamura S, Nagashima H, Kasanuki H, Takao A, et al. (1999) A novel mechanism associated with an inherited cardiac arrhythmia: defective protein trafficking by the mutant HERG (G601S) channel. *Circulation* **99**:2290–2294.
- Gong Q, Anderson CL, January CT, and Zhou Z (2002) Role of glycosylation in cell surface expression and stability of HERG potassium channels. *Am J Physiol* **283**:H77–H84.
- Gong Q, Anderson CL, January CT, and Zhou Z (2004) Pharmacological rescue of trafficking defective HERG channels formed by coassembly of wild-type and long QT mutant N470D subunits. *Am J Physiol* **287**:H652–H658.
- January CT, Gong Q, and Zhou Z (2000) Long QT syndrome: cellular basis and arrhythmia mechanisms in LQT-2. *J Cardiovasc Electrophysiol* **12**:1413–1418.
- Jones EM, Roti Roti EC, Wang J, Delfosse SA, and Robertson GA (2004) Cardiac I<sub>Kr</sub> channels minimally comprise hERG 1a and 1b subunits. *J Biol Chem* **279**:44690–44694.
- Lees-Miller JP, Duan Y, Teng GQ, and Duff HJ (2000) Molecular determinant of high-affinity dofetilide binding to HERG1 expressed in *Xenopus* oocytes: involvement of S6 sites. *Mol Pharmacol* **57**:367–374.
- Mitcheson JS, Chen J, Lin M, Culberson C, and Sanguinetti MC (2000) A structural basis for drug-induced long QT syndrome. *Proc Natl Acad Sci USA* **97**:12329–12333.
- Papazian DM, Shao XM, Seoh SA, Mock AF, Huang Y, and Wainstock DH (1995) Electrostatic interactions of S4 voltage sensor in Shaker K<sup>+</sup> channel. *Neuron* **14**:1293–1301.
- Paulussen A, Raes A, Matthijs G, Snyder DJ, Cohen N, and Aerssens J (2002) A novel mutation (T65P) in the PAS domain of the human potassium channel HERG results in the long QT syndrome by trafficking deficiency. *J Biol Chem* **277**:48610–48616.
- Petrecchia K, Atanasiu R, Akhavan A, and Shrier A (1999) N-Linked glycosylation sites determine HERG channel surface membrane expression. *J Physiol (Lond)* **515**:41–48.
- Rossenbacker T, Mubagwa K, Jongbloed RJ, Vereecke J, Devriendt K, Gewillig M, Carmeliet E, Collen D, Heidebuchel H, and Carmeliet P (2005) Novel mutation in the Per-Arnt-Sim domain of KCNH2 causes a malignant form of long-QT syndrome. *Circulation* **111**:961–968.
- Sanguinetti MC, Jiang C, Curran ME, and Keating MT (1995) A mechanistic link between an inherited and an acquired cardiac arrhythmia: HERG encodes the I<sub>Kr</sub> potassium channel. *Cell* **81**:299–307.
- Schultheis CT, Nagaya N, and Papazian DM (1998) Subunit folding and assembly steps are interspersed during Shaker potassium channel biogenesis. *J Biol Chem* **273**:26210–26217.
- Tiwari-Woodruff SK, Schultheis CT, Mock AF, and Papazian DM (1997) Electrostatic interactions between transmembrane segments mediate folding of Shaker K<sup>+</sup> channel subunits. *Biophys J* **72**:1489–1500.
- Trudeau MC, Warmke JW, Ganetzky B, and Robertson GA (1995) HERG, a human inward rectifier in the voltage-gated potassium channel family. *Science (Wash DC)* **269**:92–95.
- Zhang L, Vincent GM, Baralle M, Baralle FE, Anson BD, Benson DW, Whiting B, Timothy KW, Carlquist J, January CT, et al. (2004) An intronic mutation causes long QT syndrome. *J Am Coll Cardiol* **44**:1283–1291.
- Zhang S, Zhou Z, Gong Q, Makielski J, and January CT (1999) Mechanism of block and identification of the verapamil binding domain to HERG potassium channels. *Circ Res* **84**:989–998.
- Zhou Z, Gong Q, Epstein ML, and January CT (1998a) HERG channel dysfunction in human long QT syndrome: intracellular transport and functional defects. *J Biol Chem* **273**:21061–21066.
- Zhou Z, Gong Q, and January CT (1999) Correction of defective protein trafficking of a mutant HERG potassium channel in human long QT syndrome: pharmacological and temperature effects. *J Biol Chem* **274**:31123–31126.
- Zhou Z, Gong Q, Ye B, Fan Z, Makielski JC, Robertson GA, and January CT (1998b) Properties of HERG channels stably expressed in HEK 293 cells studied at physiological temperature. *Biophys J* **74**:230–241.

**Address correspondence to:** Dr. Craig T. January, Room 24, SMI Bldg., 1300 University Ave., University of Wisconsin, Madison, WI 53706. E-mail: ctj@medicine.wisc.edu